

A second-order cross fractal meta-material structure used in low-frequency microwave absorbing materials

Daqing Huang · Feiyu Kang · Chunlei Dong ·
Zhuohui Zhou · Xiang Liu · Heyan Ding

Received: 23 November 2013 / Accepted: 6 March 2014
© Springer-Verlag Berlin Heidelberg 2014

Abstract A second-order cross fractal meta-material structure was designed and fabricated in this project. A kind of conventional magnetic material which works at low frequency was used as the absorber substrate. The simulation results demonstrated an absorber band below –10 dB between 4 and 8 GHz, and there was a 1.7 GHz expansion when the meta-material structure was not loaded. The experiment results indicated a similar absorber band between 3 and 5.5 GHz, which was 1.09 GHz wider than meta-material structure and the absorber band expanded by 88 %. Then we further analyzed the energy distribution on the surface of the meta-material structure which perfectly explained the expansion of the absorption band and implied a way to achieve a lower wider absorber band.

1 Introduction

Microwave absorber is widely used in many different fields. With the development of detective technology, the performance of microwave absorber needs to be improved, especially when it comes to low frequency. We normally

use magnetic materials (MM) to achieve low-frequency absorption [1]. But the MM is very heavy and thick, and thus this is unacceptable in many fields.

Recently, meta-material has draw a lot of attention due to its unique properties [2]. As we all know, meta-material is a kind of artificial periodic array of metal, which can realize a negative refractive index, negative permittivity and negative permeability [3–5]. When it is used as microwave absorber, its ability of designable absorption band shows a bright future [6–8]. We can easily move the absorbing band of meta-material by adjusting the parameters of the metal structures [9]. At the same time, the electromagnetic parameters of substrate material also play a crucial role in changing the absorbing band [10]. However, meta-material has an obvious shortage. Due to its metal resonance absorption, the absorbing band is very narrow [11]. Nowadays, researchers have come up with a lot of methods to broaden the bandwidth of meta-material absorbers. The most common way is to combine a serial of different parameters of meta-materials structure to achieve a combination of different absorbing band [12–15]. This method has made certain achievements, but according to the equivalent medium theory, the number of different meta-materials structures is limited [16], especially in low-frequency band. So it is impossible to realize a wider and perfect absorber band by simply using meta-materials structure combination.

In this paper, we combined the advantages of meta-material and traditional magnetic absorbing material, focusing on using meta-material to decrease the weight and thickness of magnetic material layer and to achieve a wider absorbing band at the same time. First we designed and fabricated a second-order cross fractal meta-material structure. Then we combined it with a very thin magnetic material which is only 1 mm. The experiment results indicate that the absorbing band of 1 mm magnetic

D. Huang (✉) · F. Kang
Materials science and Engineering Department, Tsinghua
University, Beijing 100083, People's Republic of China
e-mail: hdqbiam@163.com

D. Huang · Z. Zhou · X. Liu · H. Ding
Beijing Institute of Aeronautical Materials AVIC,
Beijing 100095, People's Republic of China

C. Dong
Shenyang Institute of the AVIC, Shenyang 110035,
People's Republic of China

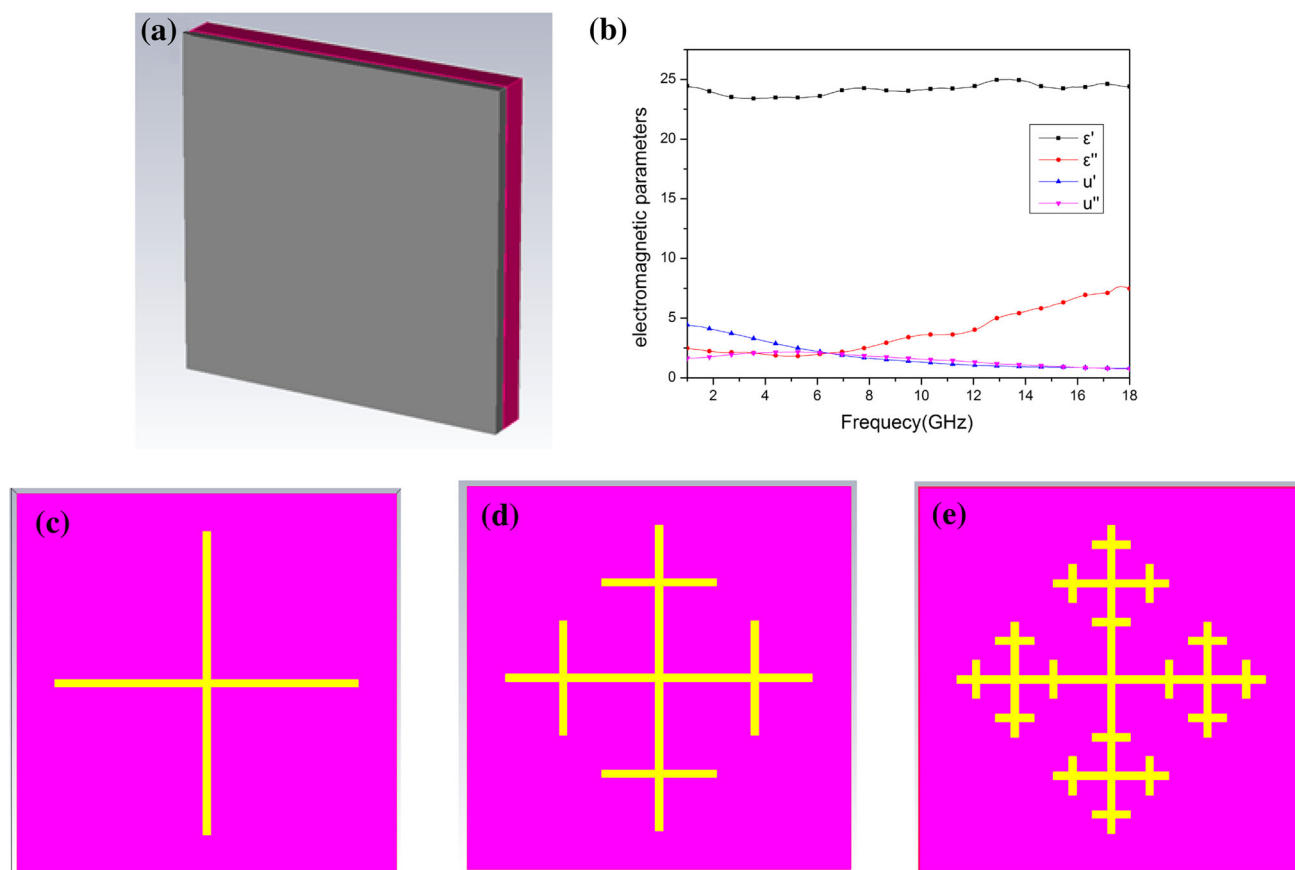


Fig. 1 different structures **a** the whole absorber structure, **b** the electromagnetic parameters of the magnetic material, **c** the first-order structure, **d** the second-order structure and **e** the third-order structure

material was moving to low frequency and compared with unloaded meta-material structure the bandwidth of the absorbing band expanded by 88 %.

2 Simulation and discussion

The fractal structure has self-similar structures which could widen the resonant bandwidth of meta-material [17]. On that case, we came up with the cross fractal structure to create a meta-material structure. The whole absorber consists of a magnetic layer, cross fractal meta-material, fr-4 substrate and metal backing from the top down, as you can see in Fig. 1a. The magnetic material's electromagnetic parameters is denoted in Fig. 1b. The red layer is fr-4 material which has a permittivity of 4.4 and a loss tangent of 0.021. Then three different cross fractal structures were designed based on their different orders, as you can see in Fig. 1c–e.

The simulation work was conducted using the commercial finite-difference time domain (FDTD) solver Microwave Studio by CST. The unit boundary condition in the x - y plane was applied. EM radiation was polarized, the

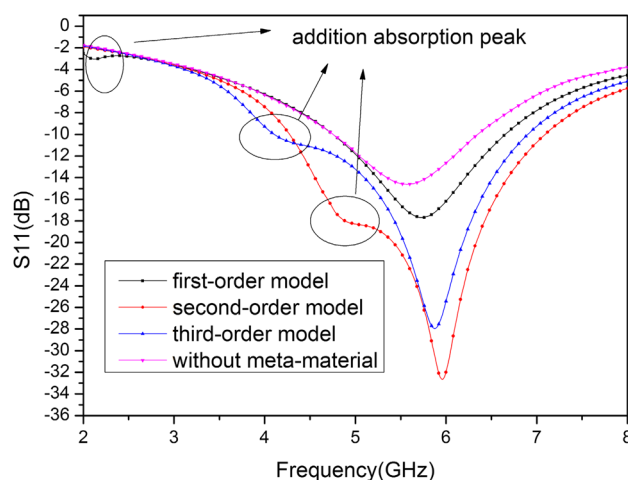


Fig. 2 S_{11} curves of different order fractal structure

wave vector was perpendicular and went to the front of the slab and the H and E fields were parallel to the X and Y directions, respectively. The simulation was performed in free space. The absorbance was calculated from the

reflectance and expressed by the S_{11} parameter as $A = 1 - S_{11}^2$ because of the metal backing. So the S_{11} curve can describe the absorption ability. Then the S_{11} parameter of those different order fractal structures was calculated and the results are demonstrated in Fig. 2.

As what is illustrated in Fig. 2, there is a main deep absorption band around 6 GHz in each fractal model which we can give credit to the MM. At the same time we found out that each fractal model has an addition absorption band,

but the position and depth are different. The addition band that is caused by the first-order cross fractal structure appears around 2 GHz and its depth is only -3 dB. The addition band that is caused by the second-order cross fractal appears around 5 GHz and its depth achieves -18 dB. The addition band that is caused by the third-order cross fractal appears around 4.5 GHz and its depth becomes -10 dB. From the analysis, we can tell that the change of the position and the depth of the addition band

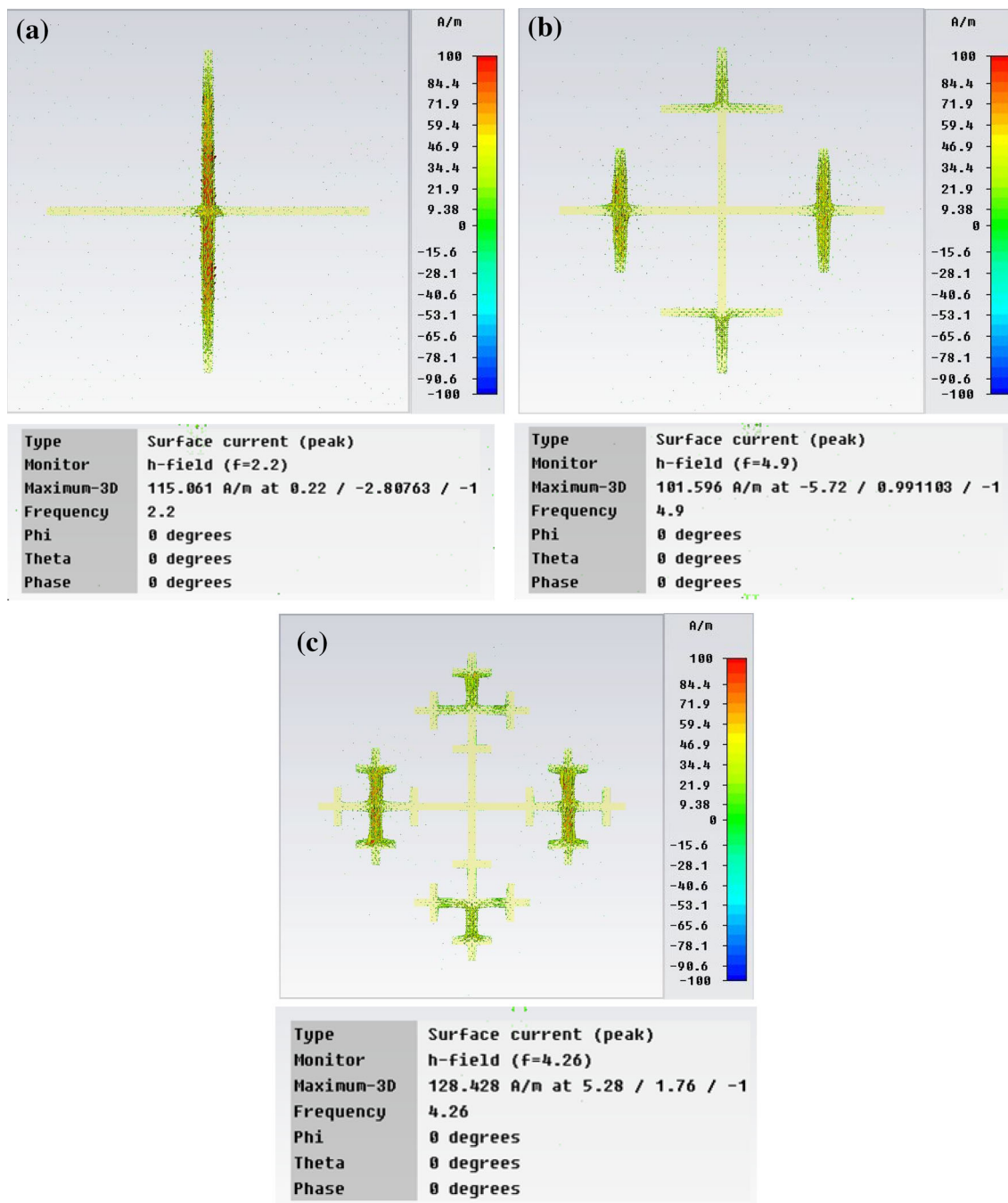


Fig. 3 The distribution of surface current a the first-order model, b the second-order model and c the third-order model

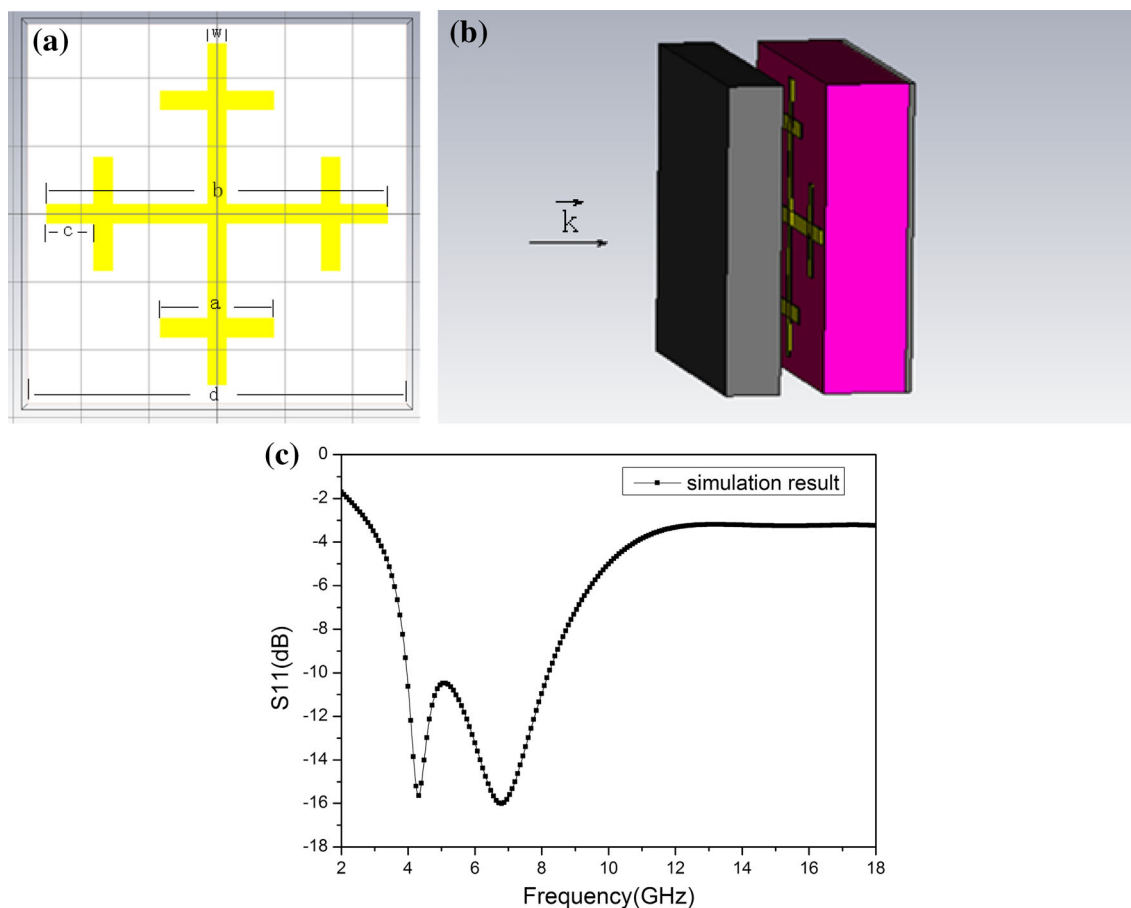


Fig. 4 Structure and its S_{11} curve: **a** meta-material structure, **b** overall configuration and **c** S_{11} curve

are not linear. With the increase of the order of the different structures, the positions of the addition absorption band become close to the main absorption band at first and then go far away from it. And the same thing happens to the depth that go deep at first then become shallow, which means the second-order structure can easily and optimally realize the expansion of the absorption band.

In order to support our conclusion, we further analyzed the distribution of the surface current around addition absorption peak, and the results are show in Fig. 3.

Figure 3 indicates two phenomena. First, the surface current mainly happens around the cross areas. Second, the distribution of surface current in second-order fractal structure is almost the same as in the third-order fractal structure. On the basis that the maximum of the surface current in both model is almost the same, we claimed that the second-order model will have stronger surface current than the first-order model since it has two cross shapes, and will have better expandable ability than the third-order model because of its deep depth of the addition peak. Based on the above analysis, we decided to use the second-cross fractal structure as the meta-material structure.

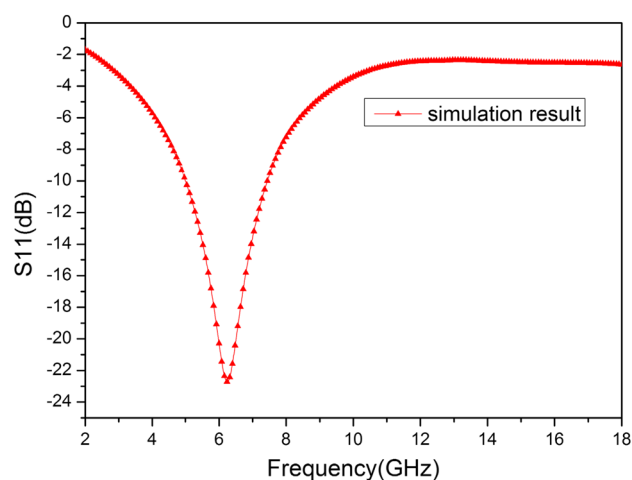


Fig. 5 S_{11} parameters of the structure without meta-material

After stimulation we have an optimized structure as displayed in Fig. 4a, and the parameters of the structure are $w = 0.28$ mm $a = 1.68$ mm $b = 5.04$ mm $c = 0.7$ mm, the unit length $d = 5.6$ mm. The total thickness of the

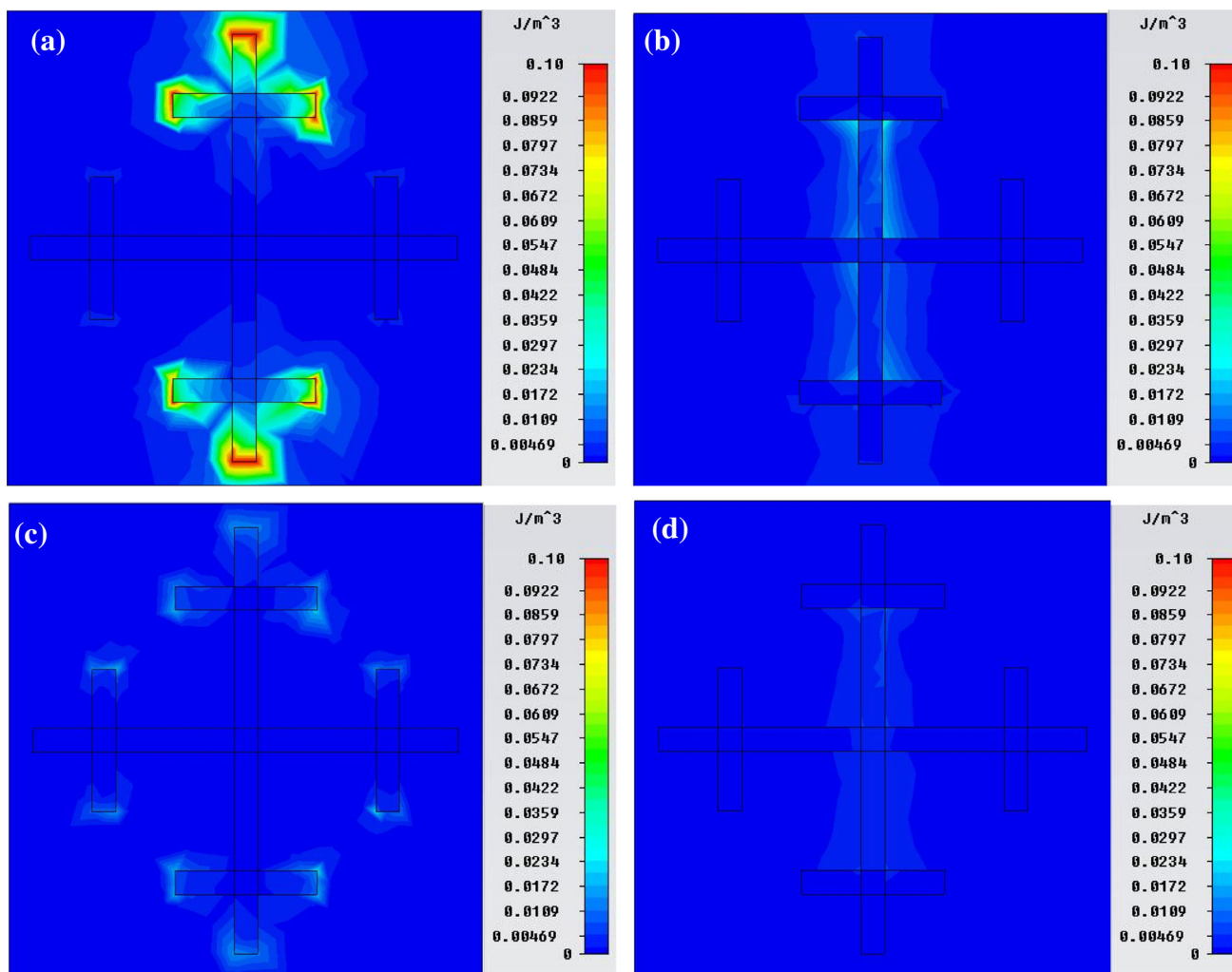


Fig. 6 Energy loss density, **a** low-frequency electric loss density **b** low-frequency magnetic loss density, **c** high-frequency electric loss density **d** high-frequency magnetic loss density

absorber is 2.6 mm. The metal backing was set as an 18 μm thick PEC film. The simulation result is illustrated in Fig. 4c.

The S_{11} curve presents a -10 dB absorption between 4 and 8 GHz. In order to reveal the influence of meta-materials, we further simulated the whole structure without the meta-material. The result is showed in Fig. 5.

Figure 5 shows an absorbing band that appears between 5.0 and 7.3 GHz which is only 2.3 GHz width. Comparing Figs. 4c and 5, we find out a double-peak absorbing band at low frequency which causes the absorbing band to expand over 1.7 GHz when the meta-material structure is loaded. In order to explore the relationship between the meta-material and the addition absorption peak, we further studied its energy loss density which includes electric energy loss density and magnetic field energy loss density at the center point of the absorption peak. The results are exhibited in Fig. 6.

According to the scale of the energy lost density, we can easily tell that the contribution of meta-material to low-frequency absorption peak is larger than that to high frequency absorption peak. And the electric loss density and magnetic loss density both demonstrate the same result. It implies that the low-frequency absorbing peak appears with the loaded of meta-material, which also moves the high-frequency absorbing peak to a higher band that further widens the absorption bandwidth. The electric loss density mainly distribute at the edges of the shape which will increase as a higher order of the fractal structure. This further explains the reason that the second-order fractal structure has a deeper and wider addition absorption peak than the first-order structure. The distributions of the electric loss density also indicated that the fractal structures have a certain contribution to the loss both at low frequency and high frequency.

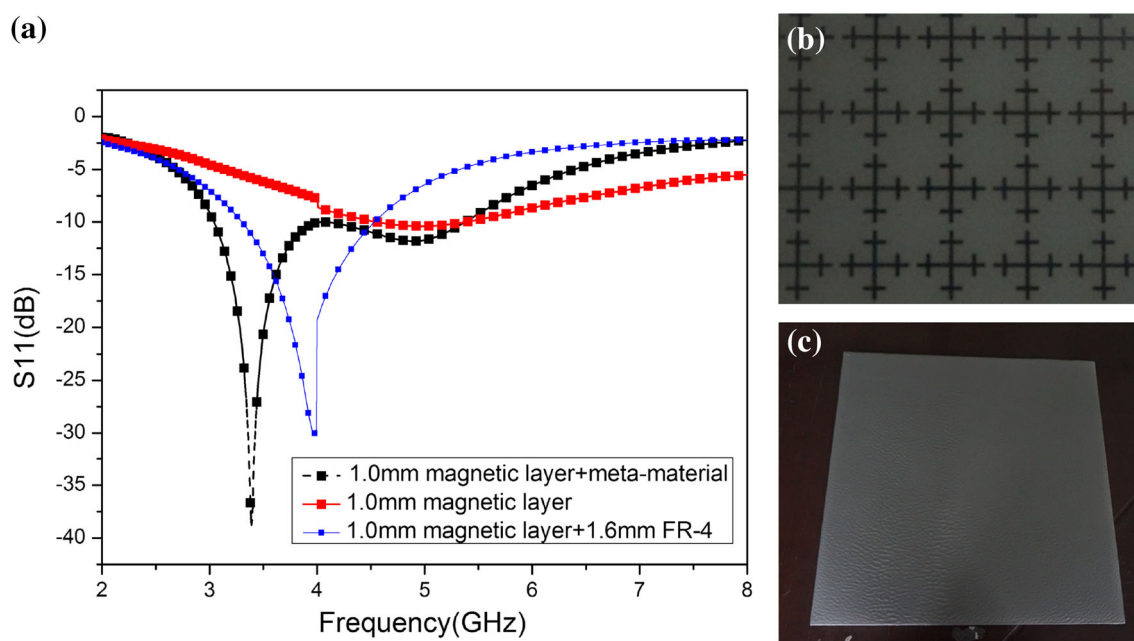


Fig. 7 Reflectivity curves and its experimental sample product: **a** the comparison chart of unloaded and loaded meta-material, **b** meta-material structure physical map and **c** sample product

3 Experiment and discussion

In order to confirm the simulation results, we adopted the PCB processing technique to manufacture the meta-material structure base on an fr-4 substrate which is 1.6 mm. On the top of the meta-material structure, a 1-mm-thick layer of magnetic absorbing material was added using the spraying process. Arched frame measurement is applied to measure the S_{11} parameters of the whole absorb structure. The results are illustrated in Fig. 7.

There is a discontinuity in the blue curve at 4 GHz in Fig. 7, which is caused by measure system since it was operated, respectively, at 2–4 and 4–8 GHz; so the S_{11} curve would have two values at 4 GHz based on different horns that were used. The red line represents the S_{11} parameter of 1 mm magnetic material which only achieves -10 dB at 5 GHz which is absolutely useless. The black line is the experiment result of the whole absorber. The absorption peak moves to low frequency and the absorption band which is below -10 dB appears from 3 to 5.3 GHz. The black line has a 1.1 GHz width absorbing band expansion compared with the blue line where the meta-material is unloaded.

According to the comparison between the experiment results and the simulation results, we can see there is a shifting of all the absorption peaks. In order to explore the reasons for this situation, we separately simulated and conducted experiments to measure the S_{11} curve of

magnetic materials absorption layer with different thicknesses and the results are demonstrated in Fig. 8.

From the comparison of simulation and experimental results of the magnetic material, we observed that the center of absorption peak of experiment results is always lower than the simulation results at the same thickness, which indicates that the errors are mainly caused by the magnetic material. We argued that there are two main reasons that lead to the differences. First, the addition material is different. The electromagnetic parameter that is used in simulation comes from the mixture of the magnetic powder and the paraffin. But in the experiment, the absorber coating is made by the magnetic powder and the epoxy resin, the permittivity of the epoxy resin is higher than the paraffin's, which will cause the permittivity of the material in the experiment being higher than that in simulation. In that case, it will further conduce to the absorption band moving to low frequency. Second, the dispersion process is different. During the measurement for the electromagnetic parameter, they mixed the magnetic powder with the paraffin only through hand stirring that will lead to bad dispersion of the magnetic powder. By contrast, the mixture of the magnetic powder and the epoxy resin in experiment is not only stirred by hand, but we also used ultrasonic and filtering to achieve a better dispersion which will contribute to a better performance at low frequency. In conclusion, the permittivity of magnetic material in experiment is higher than that in the simulation

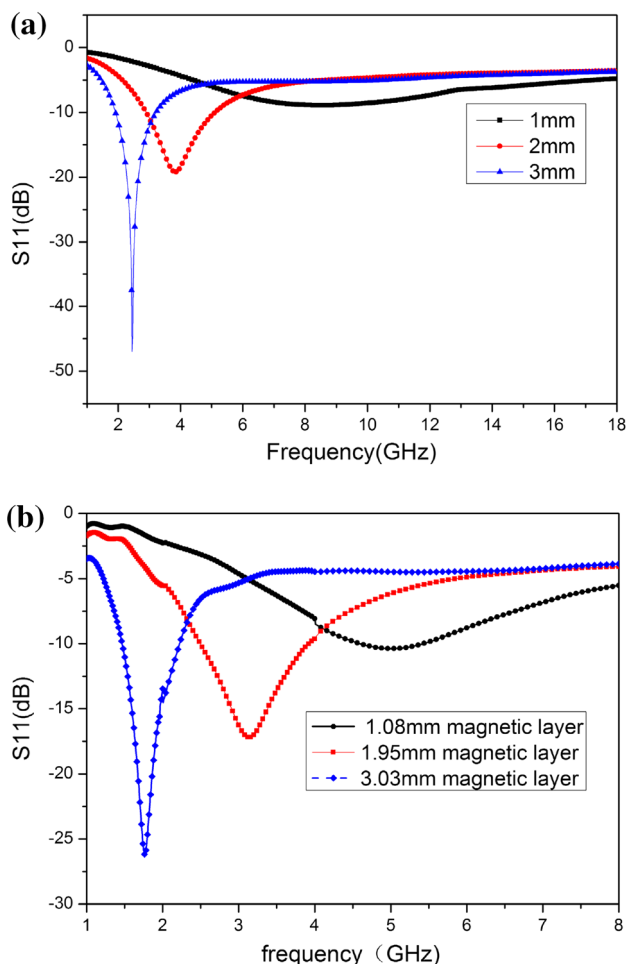


Fig. 8 S_{11} curve of magnetic absorbing materials with different thicknesses: **a** simulation results and **b** experimental results

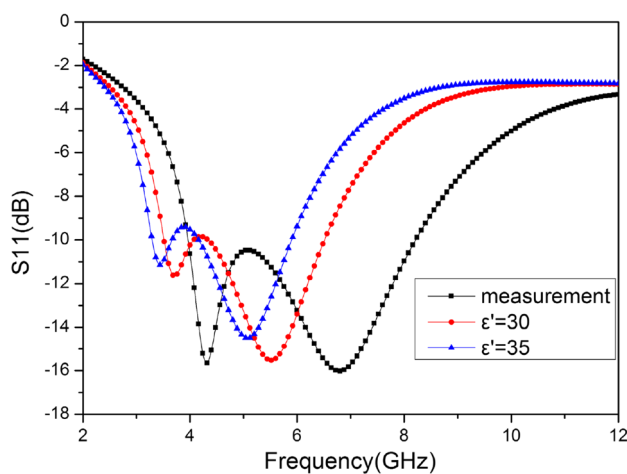


Fig. 9 S_{11} curves base on different ϵ'

because of the two reasons that result in the difference between experimental results and simulation results.

In order to support our conclusion, we gradually increased the real part of the permittivity for the magnetic material which was used in the simulation before without changing its permeability. The simulation results are presented in Fig. 9.

Figure 9 demonstrates that the dips of S_{11} curve are moving from high frequency to low frequency as the permittivity increases. When it comes to 35, the dips move to 3.4 and 5.1 GHz, respectively, which is almost the same as the experimental results. Even though the depth of the peak is not quite the same because the ϵ' is not frequency relative here, it still can explain where the differences of the simulation results and the experiment results come from. On the other hand, the trend of the change of the experimental results and the calculation results is consistent as shown in Fig. 8, and the increase of permittivity has little influence on the depth of S_{11} curve as indicated in Fig. 9, so we can conclude that the meta-material is indeed beneficial to the low-frequency band expansion.

Meanwhile, the impact of the different thicknesses of ferromagnetic absorbing layer was further explored through the experiments. The thickness of magnetic layer is set as 0.5, 1, 2 mm. The results are exhibited in Fig. 10.

As we can see from Fig. 10a, the absorption bands move from high frequency to low frequency as the thickness increases. And when it comes to 2.0 mm, the addition absorption band, represented by the blue line, almost disappears. In order to further reveal the rules that the addition absorption band obey, the experiment under the condition of unloading meta-material structure was produced as a comparison. The results are demonstrated in Fig. 10c. As it has been discussed before, the meta-material has two functions: the first one is to add an addition absorption band and the second is to slightly move the absorption band created by the magnetic material. However, combining these rules and these curves, we can see those addition absorption peaks (Fig. 10a) do not shift from high frequency to low frequency with the increasing thickness of the magnetic layer, they move to low frequency at first, then they move back and stick around at 3–5 GHz. The depths of the addition peak also go down at first, and then they go up. This indicates that the addition absorption peak has a deepest peak when the thickness is right, which indicate that we do not need to change the thickness of the magnetic material to obtain a further lower absorption band: all we need to do is change the substrate of meta-material and move the addition absorption peak to a lower frequency.

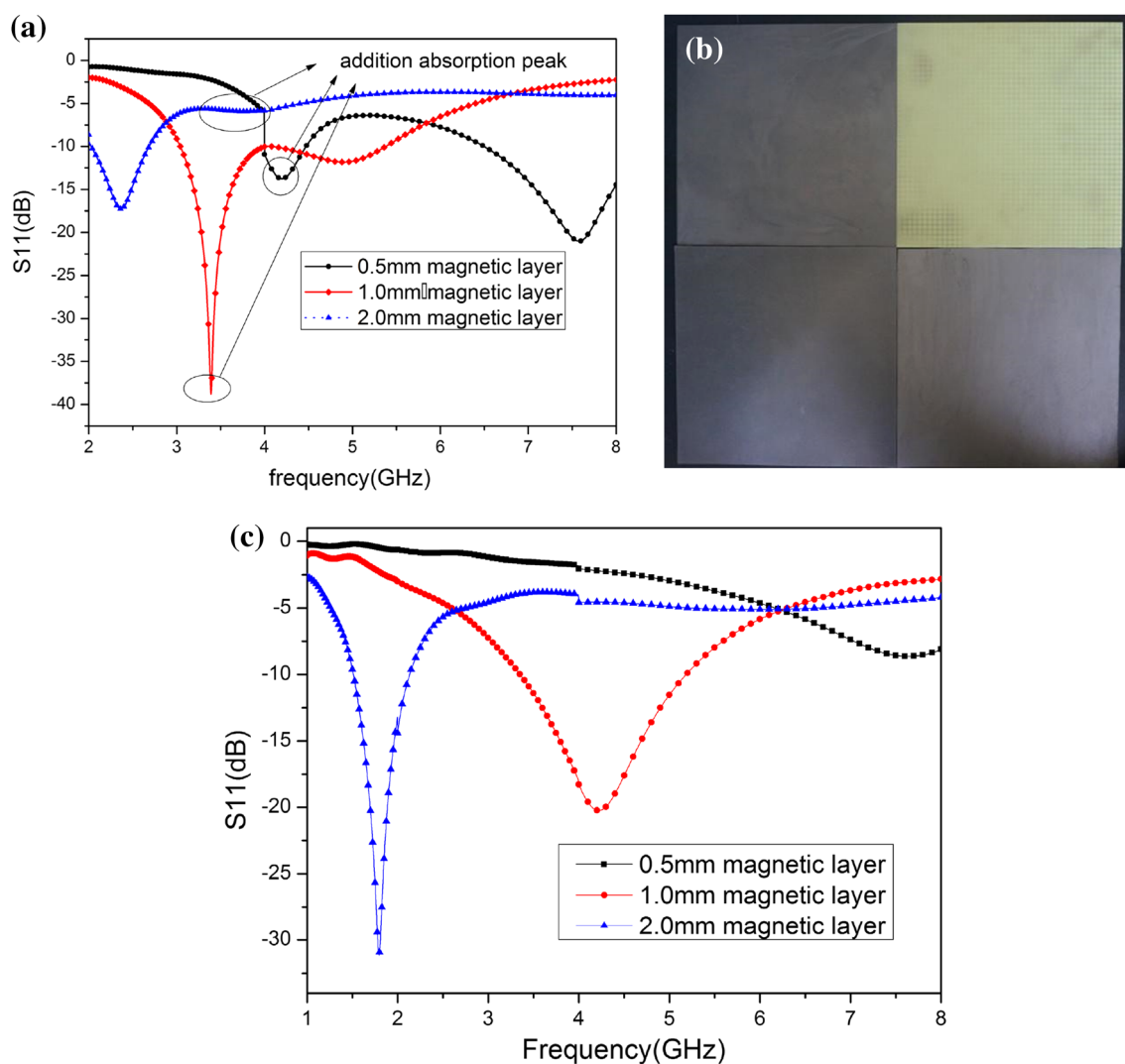


Fig. 10 Reflectivity curves and its sample product: **a** reflectivity curves of ferromagnetic absorbing materials with different thicknesses, **b** sample product and **c** different thicknesses of ferromagnetic layer without meta-material

4 Conclusion

The paper aims to use meta-material to decrease the thickness of magnetic material when it is used as low-frequency absorber, and at the same time expand the absorbing band. Both of the two goals were achieved. The thickness of the MM was decreased to 1 mm which is absolutely useless at low frequency by itself; on the other hand, the experiment results revealed that an absorber band between 3 and 5.5 GHz was 1.09 GHz wider than meta-material structure off and the absorber band expand by 88 %. In the end, the paper briefly discussed the impact of different thicknesses of the MM, and it was discovered that the addition absorption band has an deepest peak when the thickness is right, and its stability also implied a way to obtain a wide absorber band at lower frequency.

Acknowledgments This project supported by the National Defense Pre-Research Foundation of China under Grant No.9140A10 030110HK5105.

References

1. B.H. Zhang, W.D. Li, H.P. Zhou, Z. Li, M.D. Cheng, Y.H. Chen, F.D. Liang, J.L. Deng, *JAP* **113**, 013903 (2013)
2. D.R. Smith, W.J. Padilla, D.C. Vier, S.C. Nemat-Nasser, Schultz, *Phys. Rev. Lett.* **84**(18), 4184–4187 (2000)
3. J.B. Pendry, A.J. Pendry, W.J. Stewart, *Phys. Rev. Lett.* **76**(25), 4758–4776 (1996)
4. J.B. Pendry, A.J. Holden, D.J. Robbins, *J Phys.: Condens Matter* **10**, 4785–4809 (1998)
5. H.T. Chen, W.J. Padilla, J.M.O. Zide, A.C. Gossard, A.J. Taylor, *Nature* **444**, 597–600 (2006)
6. N.I. Landy, S. Sajuyigbe, J.J. Mock et al., Perfect Metamaterial Absorber. *Phys. Rev. Lett.* **100**(20), 7402–7405 (2008)

7. M F Khan, M J Mughal, 3rd International Congress on Advanced Electromagnetic Materials in Microwaves and Optics, London 30 Aug–4 Sept 522–524 (2009)
8. J.D. Baena, R. Marqués, F. Medina, J. Martel, *Phys. Rev. B* **69**(1), 014402 (2004)
9. H. Wakatsuchi, J. Paul, S. Greedy, C. Christopoulos, *IEEE Trans. Antennas Propag.* **60**, 3670 (2012)
10. X. Liu, T. Starr, A.F. Starr, W.J. Padilla, *Phys. Rev. Lett.* **104**, 207403 (2010)
11. N.I. Landy, S. Sajuyigbe, J.J. Mock, D.R. Smith, W.J. Padilla, *Phys. Rev. Lett.* **100**(20), 207402 (2008)
12. C.M. Hu Tao, D.Pilon Bingham, Kebin Fan, A C Strikwerda, D Shrekenhamer, W J Padilla, Xin Zhang and R D Averitt. *J. Phys. D Appl. Phys.* **43**(22), 225102 (2010)
13. M.H. Li, H.L. Yang, X.W. Hou, Y. Tian, D.Y. Hou, *PIER* **108**, 37–49 (2010)
14. H. Luo, T. Wang, R.Z. Gong, Y. Nie, X. Wang, *Chin. Phys. Lett.* **28**(3), 034204 (2011)
15. J. Sun, L. Liu, G. Dong, J. Zhou, *Opt. Express* **19**(22), 21155–21162 (2011)
16. Y.J. Pang, H.F. Cheng, Y.J. Zhou, J. Wang, *JAP* **113**, 114902 (2013)
17. Z.Q. Liao, R.Z. Gong, Y. Nie, T. Wang, X. Wang, *Photonic Nanostruct.* **9**, 287–294 (2011)